Supplementary Information For "Miniature Dungey-like cycle at Mars: a new twist on an old auroral paradigm"

Shaosui Xu[1*], James P. McFadden[1], David L. Mitchell[1], Janet G. Luhmann[1], Jasper S. Halekas[2], Kathleen G. Hanley[1], Christian X. Mazelle[3], Jared R. Espley[4], Shannon M. Curry[5]

[1]Space Sciences Laboratory, University of California Berkeley, 7 Gauss Way, Berkeley, 94720, California, USA.
[2]Department of Physics and Astronomy, University of Iowa, Iowa City, Iowa, USA.
[3]IRAP, CNRS - University of Toulouse - UPS - CNES, Toulouse, France.
[4]Goddard Space Flight Center, Greenbelt, Maryland,USA.
[5]Department of Astrophysical and Planetary Sciences, University of Colorado Boulder, 2000 Colorado Ave, Boulder, 80305, Colorado, USA.

*Corresponding author(s). E-mail(s): shaosui.xu@ssl.berkeley.edu;
Contributing authors: mcfadden@ssl.berkeley.edu; mitchell@ssl.berkeley.edu; jgluhman@ssl.berkeley.edu; jasper-halekas@uiowa.edu; gwen.hanley@berkeley.edu; cmazelle@irap.omp.eu; jared.Espley@nasa.gov; shannon.curry@colorado.edu;

Contents of this file

Supplementary Figure S1

Supplementary Figure S2

Supplementary Figure S3

Introduction

This document encloses supplementary figures for the manuscript "Miniature Dungey-like cycle at Mars: a new twist on an old auroral paradigm"

More detailed MAVEN observations. Figure S1 shows more detailed information for the case study in the main text. Particularly, the calculation of $\mathbf{B^r}$ relies on the estimation of the unperturbed intrinsic crustal magnetic fields $\mathbf{B_c}$. As this study focuses on some of the strongest crustal fields at Mars that are well captured by crustal field models, we use the adjusted modeled crustal field [**?**] as the baseline to be subtracted from the observed magnetic fields $\mathbf{B_{obs}}$ to obtain $\mathbf{B^r}$. To capture small-scale magnetic perturbations caused by FACs, adjustments to the modeled crustal field are needed to remove the possible (spatially) large-scale induced magnetic fields from the interaction between Mars and the solar wind. We first obtain linear fits between the observed and modeled magnetic fields for each vector component within 5 minutes bracketing the time of interest. We then recalculate and adjust the "modeled" fields ($\mathbf{B'_c}$, dashed lines in Figure S1b) using these linear fits to capture the smooth variation of the observed magnetic fields, which include both the crustal fields and the large-scale induced magnetic fields. We illustrate the comparison of the observed and adjusted modeled field component in the east-west direction in Panel c to better highlight the main magnetic perturbation. The difference between the observed and adjusted "modeled" fields $\mathbf{B^r} = \mathbf{B_{obs}} - \mathbf{B'_c}$ (Figure S1d) reflects the perturbations from currents. Indeed, the calculated $\mathbf{B^r}$ is mostly zero except in the vicinity of accelerated electrons. Note that the magnetic field data in this figure and the main text are in 1-s resolution.

Calculation of the current density from magnetic perturbation $j^b_{//}$. By assuming a field-aligned current sheet along the east-west direction and the spacecraft moving mainly from north to south, we can derive the a current density mainly in the radial direction $j_r = \frac{1}{\mu_0}\frac{\Delta B^r_{EW}}{dL_{NS}}$, where $\Delta B^r_{EW} = B^r_{EW}[t] - B^r_{EW}[t-1]$ is the difference in B^r_{EW} between two time steps and dL_{NS}=$L_{NS}[t] - L_{NS}[t-1]$ is the spacecraft motion in the north-south direction between two time steps. Then the field-aligned component of the current, FAC, is calculated as $j^b_{//} = j_r \cdot |b_r|$, where $|b_r|$ is the absolute value of the radial component of the unit vector of the measured magnetic field. The absolute value of b_r is used so that the sign of FAC refers to upward ($j^b_{//} > 0$) or downward ($j^b_{//} < 0$) FAC with respect to the local plane, rather than the local magnetic field. The calculated $j^b_{//}$ is shown as the blue line in Figure S1e.

Calculation of the current density from electrons $j^e_{//}$. The electron current density is calculated from MAVEN SWEA measurements as: $j^e_{//} = -e \iint f[E,\theta] \sin\theta \cos\theta 2\pi \, dE \, d\theta$, where $f[E,\theta]$ is the electron differential number flux in the unit of $cm^{-2}s^{-1}sr^{-1}eV^{-1}$ and e is the elementary charge. θ is the adjusted pitch angle, the angle between electron velocity and $-|b_r|$, so that $\theta < 90°$ refers to downgoing electrons and $\theta > 90°$ upgoing electrons. This is to have the sign of $j^e_{//}$ also

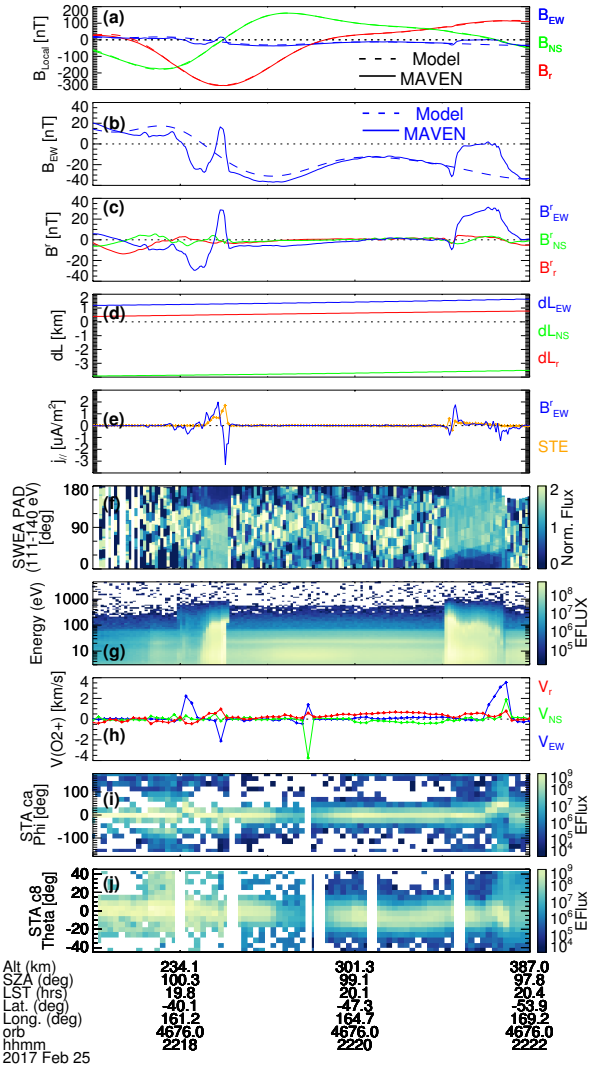

Fig. 1 Figure S1. More detailed MAVEN observations on 27 February 2019. Time series of (a) measured (solid) and modeled (dashed) magnetic field vectors in the local horizontal plane, (b) measured (solid) and adjusted modeled (dashed) magnetic field in the east-west direction, (c) magnetic residual $\mathbf{B^r}$ in the local horizontal plane, (d) spacecraft movement $\mathbf{dL}$ in the local horizontal plane, (e) field-aligned current density $j_{//}$ estimated from magnetic pertubation B^r_{EW} (blue) and superthermal electron fluxes (orange), (f) normalized electron pitch angle distributions at 111-141 eV by the averaged energy flux of each measurement, (g) superthermal electron energy-flux spectra, (h) the flow velocity of $O_2{}^+$ ($\mathbf{V}(O_2{}^+)$), the angular distribution of ions in the instrument (i) ϕ (anodes) and (j) θ (deflection) directions.

refer to upward or downward FAC to be consistent with $j^b_{//}$. The integration of energy excludes electrons below 20 eV, as these electrons may include secondary electrons produced by precipitating electrons impacting the atmosphere and interior surfaces of the electron instrument. The calculated $j^e_{//}$ is shown as the orange line in Figure S1e.

Calculation of flow velocity of O_2^+. The flow velocity is derived from the MAVEN STATIC measurements, after correcting for the spacecraft velocity and spacecraft potential. The flow velocity of O^+ is also calculated and is very similar to that of O_2^+, thus not shown for simplicity. The ion distributions are mostly broad in angular distributions, as shown in Figures S1i and j, and clear deflections from the ram direction are observed in the instrument ϕ direction (Panel i), so that the flow calculation for this case study is robust.

Zoomed-in views of MAVEN observations on 27 February 2019. Figures S2 and S3 show the zoomed-in views of the MAVEN observations for the two time periods of electron acceleration, respectively. In both figures, we now use the 32-Hz magnetic field data from MAVEN-MAG to highlight some rapid variations in the magnetic perturbation (Panel c) and thus the calculated $j^b_{//}$ (Panel e).

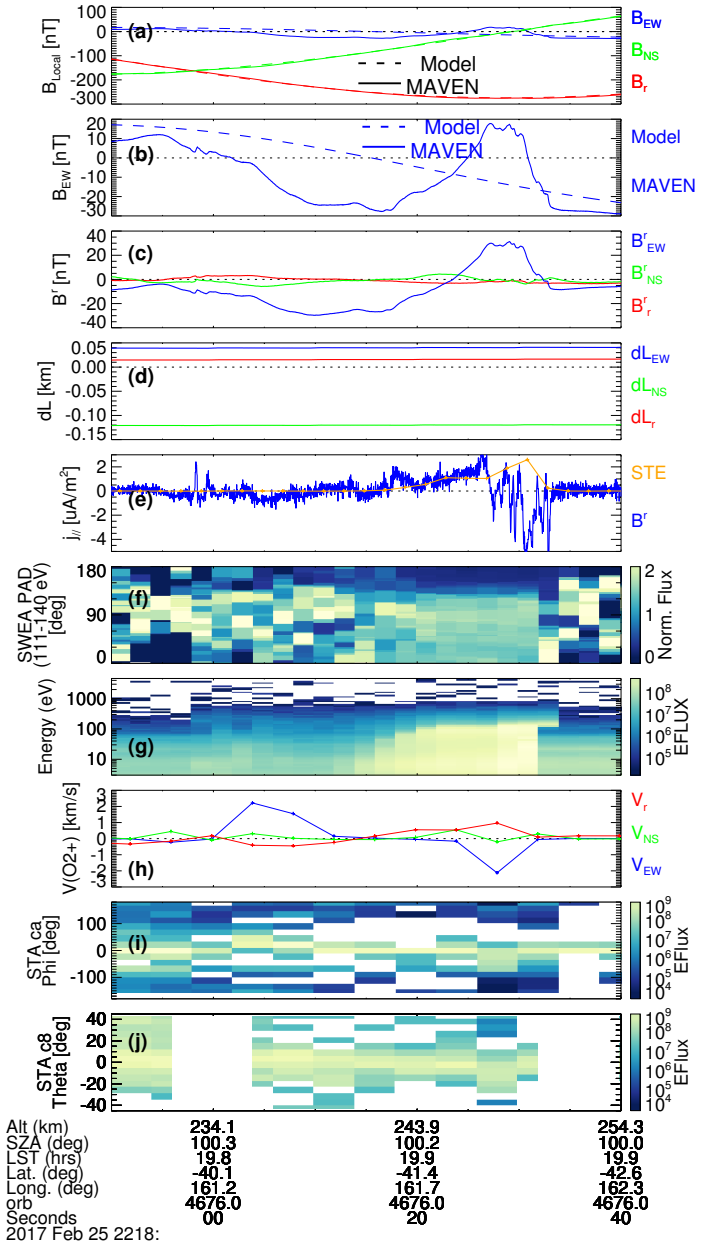

Fig. 2 Figure S2. A zoomed-in view of MAVEN observations at 22:18 UT. A zoomed-in view of MAVEN observations at around 22:18 UT with the same format as Figure 1.

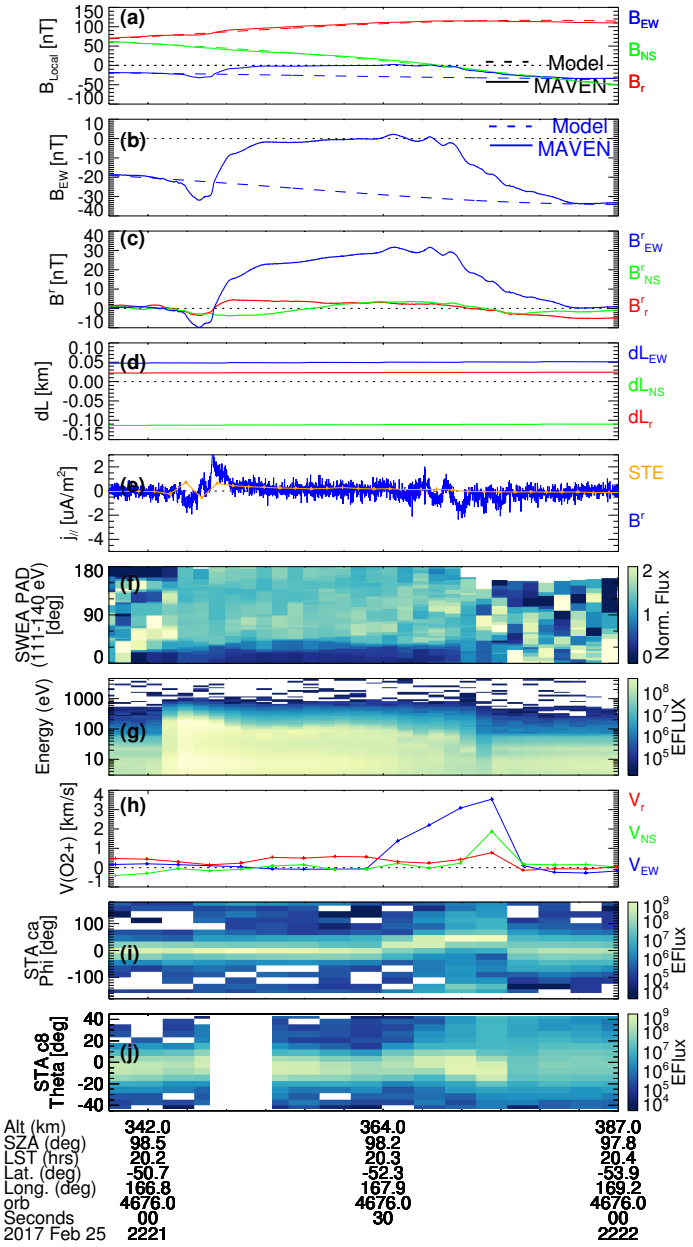

Fig. 3 Figure S3. A zoomed-in view of MAVEN observations at 22:21 UT. A zoomed-in view of MAVEN observations at 22:21 UT with the same format as Figure 1.